



Original Research Article

Au Decorated Mesoporous TiO₂ as a High Performance Photocatalyst towards Crystal Violet Dye

Simin Janitabar Darzi^{1*} , Hajie Bastami²

¹ Materials and Nuclear Fuel Research School, Nuclear Science & Technology Research Institute, Tehran, Iran

² Department of Materials and Metallurgical Engineering, Technical and Vocational University (TVU), Tehran, Iran

ARTICLE INFO

Article history

Submitted: 19 September 2021

Revised: 03 October 2021

Accepted: 20 October 2021

Available online: 26 October 2021

Manuscript ID: [AJCA-2109-1281](#)

Checked for Plagiarism: Yes

DOI: [10.22034/AJCA.2021.305643.1281](#)

KEYWORDS

N-demethylation

Photocatalytic Degradation

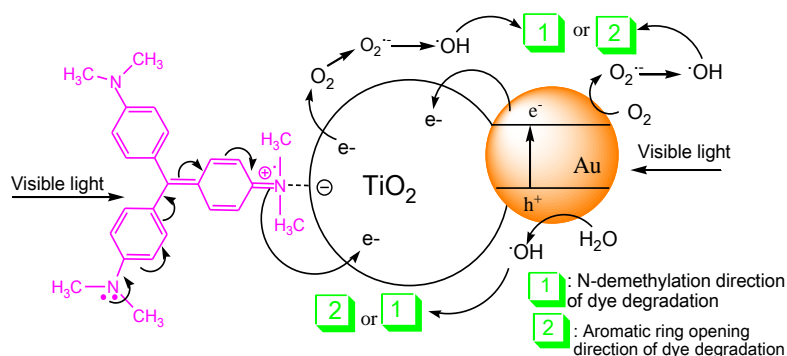
Surface Plasmon Resonance

Visible Light

ABSTRACT

Sol-gel derived TiO₂ was prepared and decorated with Au nanoparticles by photo deposition technique and examined by means of TEM, XRD, EDX, DRS, and BET-BJH analyses. The band gap was related to the Au decorated TiO₂ (Au/T) and the synthesized plain TiO₂ were obtained from DRS curves by 3.07 and 3.2 eV. The Au/T showed an enhanced visible light photocatalytic activity towards the Crystal violet (CV) dye in comparison to the plain TiO₂ because of surface plasmon resonance phenomenon of the gold nanoparticles. A cooperative working mechanism involving the possible photoactivation of gold nanoparticles as well as surface bounded dye was proposed for the photocatalytic performance of Au/TiO₂ system. During the decolorization of the CV dye, two reaction pathways including demethylation of amine sites of the chromophore system and breaking of the whole conjugated chromophore skeleton competing each other. The demethylation of amine sites of CV dye took place predominantly through the raid of OH species to the dye N, N-dimethyl groups, in a stepwise manner.

GRAPHICAL ABSTRACT



Photoactivation of dye and plasmonic Au followed by N-demethylation and cleavage of dye aromatic rings is proposed for higher photocatalytic activity of Au/TiO₂

* Corresponding author: Janitabar Darzi, S.

✉ E-mail: sjanitabar@aeoi.org.ir

© 2022 by SPC (Sami Publishing Company)

Introduction

In recent years, research on TiO_2 semiconductor has grown considerably not only for its merits as a photocatalyst, but also for its facile production, inexpensiveness, biological and photochemical stabilities. However, due to intrinsic shortcomings of TiO_2 such as fast hole-electron recombination and restricted absorption of photons in the visible range, its application in industry is limited [1, 2]. Recently, many efforts have been made to apply TiO_2 more efficiently under illumination of visible light in order to utilize solar spectrum. According to experimental findings, the existence of doped non-metal or metal species in TiO_2 surface promotes its photocatalytic performance. Notwithstanding, the fact that doping by nonmetal species expands the photoactivity of TiO_2 into the visible light range, it may be diminishing the quantum yields of this mater [3].

Another strategy considered as a useful manner for improving the TiO_2 activity is doping with noble metals such as Pt, Ag, Au and Pd which has been reported widely in recent years. The Noble metals with surface plasmon resonance (SPR) properties are envisaged not only to enhance visible light absorption but also to minimize hole-electron recombination process. Semiconductors coupled with plasmonic Au nanoparticles have been found to catalyze the epoxidation of propylene, NO reduction, many hydrogenation reactions, the oxidation of alkanes, and the water-gas shift reaction [3, 4].

In this study, Au decorated mesoporous anatase titanium dioxide was fabricated by a novel simple photo deposition technique. The photocatalytic activity of prepared Au decorated TiO_2 in comparison to pure TiO_2 was investigated for photocatalytic decomposition of an aqueous solution of the Crystal violet (CV: N, N, N',N',N'',N''- hexamethyl pararosaniline) dye. CV is a common dye of triphenylmethane, which is widely used as a dermatological agent, biological

stain, additive to poultry fees to prevent the spread of ugly bacteria, veterinary drugs also as a mercantile textile dye. Since CV is a mitotic poison and mutagen, a lot of scientific efforts such as photocatalytic experiments have been performed for the degradation of this dye. There is a great concern about the photocatalytic decomposition of the triphenylmethane dyes category because of probability of producing some harmful intermediates. The photocatalytic reactions can produce some N-dealkylated aromatic amines which are similar to the carcinogen aromatic amines in term of structure [5, 6].

There is the lack of sufficient information about the mechanism of CV decolorization and its probable intermediates in pathway of degradation. In this research, the pathway of photo decolorization of CV dye at the surface of the prepared plain and Au decorated TiO_2 photocatalysts was proposed and investigated in mechanism point of view.

Experimental

Materials and Methods

The chemicals used for this work were urea, AgNO_3 , Crystal violet, and ethanol, hydrochloroauric acid, and titanium tetrachloride. All Chemicals were analytical graded without further purification.

Plain TiO_2 was synthesised by sol-gel technique. First, 1 mL of TiCl_4 under constantly stirring was subjected to 100 mL of H_2O in an ice water bath. Then, a proper amount of urea was poured to the reaction container and stirred at 103 °C for 7 h. The precipitate was centrifuged and washed with dionized water. After washing, no Cl^- ion was detected by the reaction with 0.1 N AgNO_3 solution. The product was dried at 100 °C and calcined at 445 °C for 5 h. The produced powder was named T.

Au/T photocatalyst was prepared by the photoreduction method as follows: 0.5 g of the

synthesized titanium dioxide (T) was added to 100 mL of 20% ethanolic solution of 7.15×10^{-5} mol L⁻¹ of H₂AuCl₄ under vigorous stirring for 5 h under ultra violet illumination. Afterwards, the sample was centrifuged, washed by dionized water, and then dried at room temperature. The prepared nanopowder was named Au/T.

Photocatalytic performance testing

Photocatalytic performance of T and Au/T samples was examined by the Crystal violet dye degradation under visible light. Photocatalytic tests were carried out in a 100 mL capacity open Pyrex container. An Osram lamp was used as radiation source and distance between the lamp and reaction container was adjusted at 15 cm. During the reaction, the amount of oxygen existing in the container was held fixed by means of an aquarium pump. The set-up was cooled with a fan and all of the tests were done at about 25 °C. For all experiments, the photocatalyst amount was 1 gL⁻¹ and the concentration of dye was 5 ppm. Prior to starting the photocatalytic reaction, the suspension was stirred in the dark for 30 minutes to guarantee an adsorption-desorption equilibrium among the oxygen, the photocatalyst, and dye molecules. After regular intervals during the photocatalytic reaction, about 5 mL of suspension was picked up and centrifuged. After that, the filtrates were subjected for studding by means of Uv-Vis spectroscopy.

Results and discussion

Characterization of the products

X-ray diffraction measurements were applied to investigate crystalline structures of T and Au/T samples. The XRD patterns of Au/T and T samples are presented in Figure 1. The diffraction peaks of the plain T and Au/T confirmed the tetragonal anatase. The average crystallite size of T and Au/T samples, calculated

by the Scherrer's method, were 9.0 nm and 15.4 nm. Some new weak peaks at $2\theta = 38.2^\circ$, 44.4° and 64.6° were observed in XRD pattern of Au/T sample compared with that of T-sample, which can be ascribed to the diffraction peaks of (111), (200), and (220) planes of polycrystalline Au, respectively [7, 8].

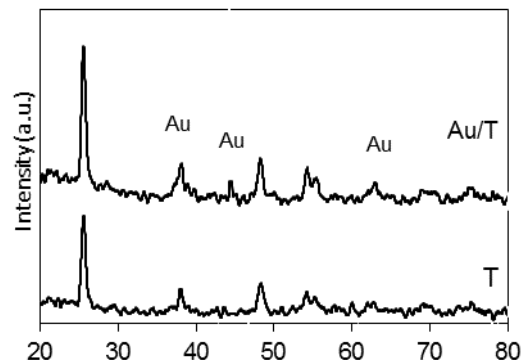


Figure 1. XRD patterns related to the synthesized T and Au/T

TEM images of T and Au/T samples and their corresponding SAED patterns are shown in Figure 2, where both of T and Au/T powders have grainy agglomerated structure and the prepared Au/T powder is more agglomerated than that of T.

The SAED pattern of the plain T and Au/T nanoparticles revealed the formation of entirely separated concentric rings indicating their high crystalline nature, and clearly illustrating that the structural integrity of titanium dioxide is maintained after anchoring of gold onto the surface of TiO₂. The diffraction peaks of planes of T and Au/T polycrystalline of TEM are in accordance with XRD ones.

Energy-dispersive X-ray (EDX) pattern (Figure 3) showed Au/T contains of Ti, O and small amount of Au. The amount of gold in the Au/T was calculated and it was 1 wt%.

Figure 4 shows Uv-DRS spectra of T and Au/T samples. The DRS spectra of the matter were obtained by absorbance mode. No absorption band in the visible region was observed for T contributed to the gold characteristic surface plasmon resonance absorption [9, 10]. Surface

plasmon resonance effect was attributed to the sample while Au/T sample exhibited a prominent

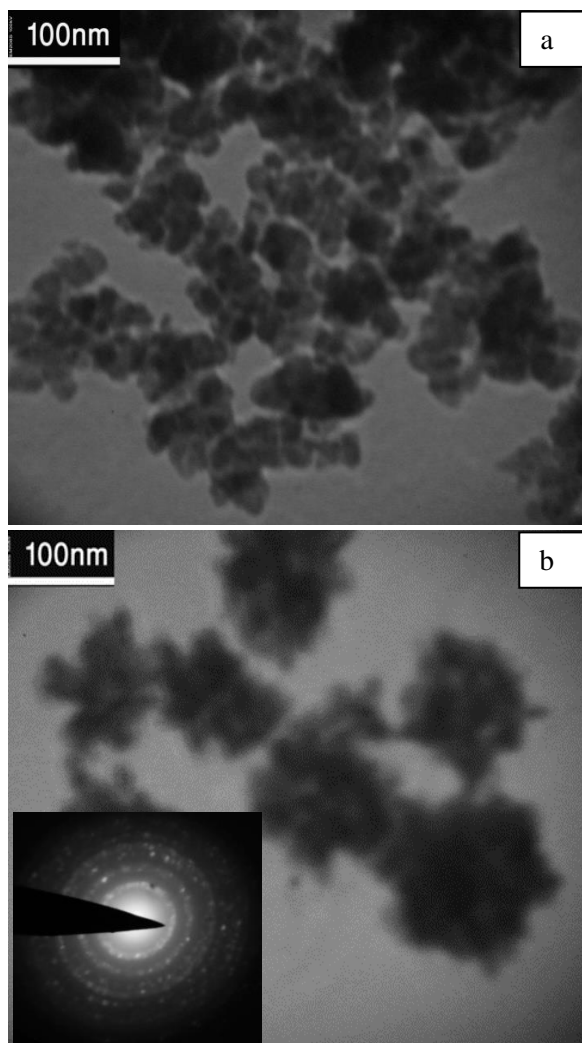


Figure 2. The images of TEM analysis for T(a) and Au/T (b) samples, and their related SAED patterns

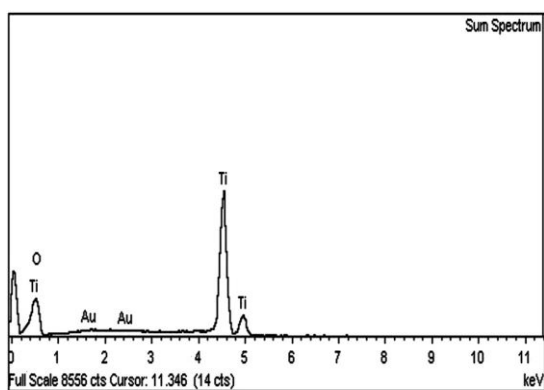


Figure 3. EDX spectroscopy analysis of Au/T

plasmon approximately at 555 nm. This emergence of electrons and photons at nanoscale dimension. The surface plasmon resonance absorption of the gold nanoparticles appeared from the excitation of electrons at 6sp level. The excited intra-band electrons migrated to the conducting band of titanium dioxide because of the surface plasmon resonance effect [11].

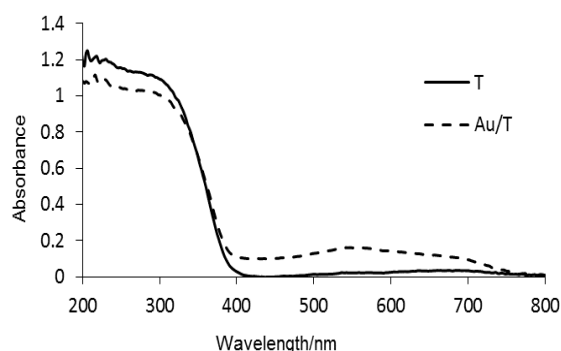


Figure 4. DRS spectra of T and Au/T

The high visible light absorption capacity of Au/T is of great importance for its photocatalytic application. The band gap energy of the prepared materials was obtained from the straight section of the DRS curves using $E_g = 1240 \lambda^{-1}$ equation, where λ is optical absorption edge of materials in Uv-Vis spectrum [12]. By this technique, the optical band gaps of Au/T and T samples was determined as 3.07 eV and 3.2 eV, respectively. A marked shift of the absorption edge towards the higher wavelength, was shown by comparing the curves of T and Au/T, confirming the introducing Au onto the surface of titanium dioxide.

Figure 5 reveals Brunauer-Emmett-Teller (BET) surface area analysis and the corresponding Barrett-Joyner-Halenda (BJH) pore size distribution plot (inset) for T and Au/T samples. Due to the presence of meso size pores in the prepared samples, isotherms of IV type were observed [12]. The triangular shape of hysteresis loop with a steep desorption branch of the samples is ascribed to the classification of H_2 type. Such hysteresis loops are attributed to the porous materials with pore shapes of ink-bottle

like which have also pore connectivity property. [13-15]. The BET surface areas of T and Au/T samples were calculated to be 186.9 and 153.1 m^2g^{-1} , respectively. Moreover, according to their BJH plot, the mean pore sizes were 6.12 and 3.62 nm for T and Au/T, respectively. The lower surface area and pore diameter of the Au/T in comparison with T sample could be due to the contraction of pores because of the insertion metallic nanoparticles in the pores.

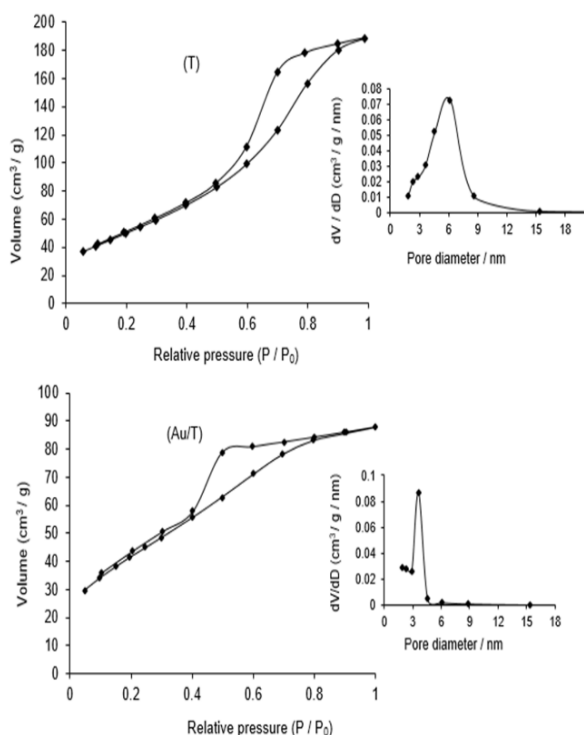


Figure 5. BET N_2 -adsorption-desorption isotherms and BJH pore size distribution plot (insets) for the mesoporous T and Au/T samples

Photocatalytic activity and proposed mechanism of CV degradation

Figures 6a and b display the spectral changes taking place through the degradation of CV at the surface of T and Au/T photocatalysts under visible light irradiation.

As shown in Figures 6 a and b, the maximum absorption (λ_{max}) of the dye is observed at 588.5 nm and the intensity of spectra is decreased with a huge hypsochromic shift in λ

max in both of Au/T and T photocatalytic systems. Generally, the wavelength of light that dye chromophore absorbs is depended on how conjugated the molecule is. If the amount of conjugation in the chromophore system is reduced, a hypsochromic shift in the UV-Vis spectrum will happen. On the other side, according to the literature, when triphenylmethane dyes undergo a photocatalytic degradation, the process of demethylation of amine sites in the chromophore system can occur [16, 17]. It seems that during the decolorization of the CV dye, two reaction pathways including demethylation of amine sites of the chromophore system and breaking of the whole conjugated chromophore skeleton simultaneously takes place. Some reports have acknowledged that a competition between N-demethylation reaction and cleavage of conjugated structure exists [17]. The N-demethylation of CV dye will be performed in a stepwise demeanor to produce mono-, di-, tri-, tetra-, penta-, and hexa-N-demethylated intermediates. The CV dye has six methyl groups at three different amine site. There are two different isomers of di-N-demethylated type intermediates, which differ from each other because of their various kinds of methyl losing from the amine sites. The di-N-demethylated isomers have four methyl groups due to losing two methyl groups from plain CV. If one methyl group separates from one of amine groups of the CV molecule and the second methyl is removed from another amine site of the dye molecule, and DMPR is produced. Nevertheless, if removing of both of two methyl groups originate from one amine site, DDPR species is produced. By losing three methyl groups, some different new species are probable for appearing. If each of the three methyl groups can be removed from distinct amine sites, the prepared tri-N-demethylated CV isomer will be MMMPR. DMPR isomer is formed by eliminating of two methyl groups from the one amine sites of the dye, while the latest separated methyl is removed from another

amine group. Both of DPR and MMPR isomers have lost four methyl groups from the plain CV structure. The DPR is formed by removing of four methyl groups from two amine sites of the plain CV molecule.

However, MMPR is produced by eliminating of two methyl groups from one of amin sites of the CV and simultaneously removing of the other two methyl groups from two distinct amine groups in the dye. Lu *et al.* [18] propounded above terms and reported maximum absorption wavelength (λ_{max}) of some N-demethylated species of the CV. According to the literature, λ_{max} of CV (N,N,N',N',N'',N''-Hexamethylpararosaniline or DDDPR), DDMPR, DMMPR, DDPR, MMMPR, DMPR, MMPR, DPR, MPR, and PR (Pararosaniline or hexa-N-demethylated CV) are located at 588.5, 581.0, 579.8, 573.7, 570.0, 566.3, 566.3, 561.5, 554.1, and 543.2 nm, respectively [18]. These reported λ_{max} related to the different intermediates in photodegradation of CV dye

were also observed in the absorbance spectra of this dye during our photocatalytic experiments under visible light on the surface of T and Au/T (Figure 6a and 6b).

According to Figures 6a and b, the maximum absorption wavelength for the N-demethylated dye species appear with a significant hypsochromic shift compared to λ_{max} of plain CV. Considering the maximum absorption wavelengths observed in the Figures 6 a and b, producing of some intermediate species such as DDPR, DMMPR, DMPR, MMMPR, MPR and PR is confirmed. Moreover, the intensity of Uv-Vis spectra of dye decreased to the amount of 22.5 and 23.3% after the addition of TiO_2 and Au/ TiO_2 , respectively, which is reflecting the adsorption ability of each of photocatalysts in the dark. The dye molecules are adsorbed onto the T or Au/T surface through the interaction between positive charge of dimethylamine groups and the hydroxyl groups at the surface of the photocatalysts. According to the photocatalytic experiment, Au/T exhibits superior visible light photocatalytic activity toward the dye in comparison to the plain TiO_2 . During the course of 120 minutes of photocatalytic experiment, the CV dye was completely decolorized on the surface of the Au/T catalyst. Although the specific surface area of Au/T sample is not higher than that of T, its photocatalytic activity is superior. The better efficiency of Au/T could be attributed to more photon absorption ability of Au/T sample in the visible region.

Using the experimental results, the pathway of CV degradation is proposed and schematically presented in Figure 7. Under irradiation of visible light, electrons as well as dye radical cations ($\text{dye}^{\bullet+}$) trapped in surface states are generated. The electrons which exist at the surface of the titanium dioxide may be scavenged by the adsorbed oxygen at the surface of TiO_2 to form superoxide radical anions which can finally produce hydroxyl radicals by bearing on one-electron reduction process [19]

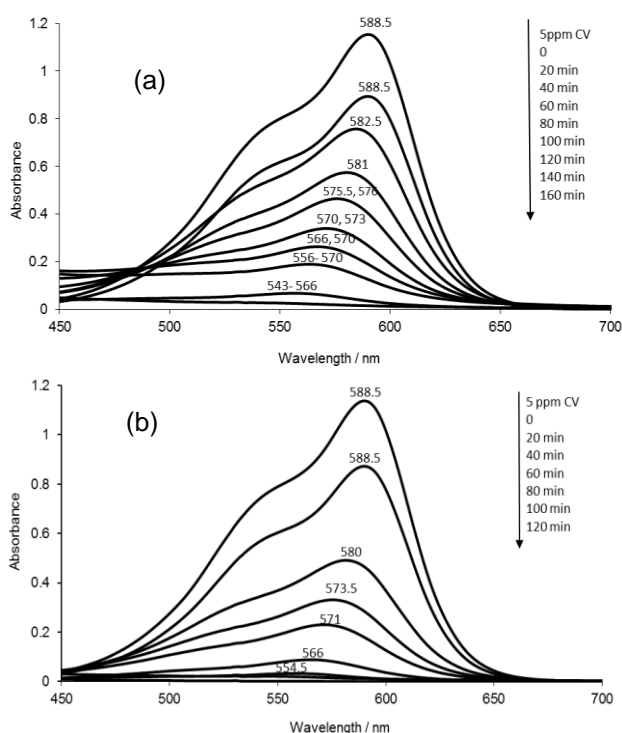


Figure 6. Changes in the absorbance spectra of CV dye during visible light degradation at the surface of T (a) and Au/T (b)

The demethylation of amine of CV dye takes place frequently through the attack of hydroxyl radicals to the N,N-dimethyl sites of the dye (pathway 1). At this pathway, the formation of nitrogen-centered radicals is probable. This phenomenon is in accordance with the earlier reports [20, 21]. The dye radical cation finally reacts with molecular oxygen or reactive oxygen radicals to form other radicals or some intermediate species. At this stage, mineralization of dye will be possible if secondary radical process occurs. On the other side, the $\cdot\text{OH}$ radicals, as main oxidizing agents, can attack the CV in pathway 2 resulting in the degradation of dye by the decomposition of the coherent aromatic ring system and opening of conjugated skeleton [22]. By utilizing the Au/T visible light photocatalytic system, the Au nanoparticles could also be photo-excited regarding their surface plasmon resonance and

provide a new way for electrons and holes generation [21, 11]. The surface electrons of the excited Au sites can react with oxygen to produce the superoxide radical anion $\text{O}_2^{\cdot-}$ and finally $\cdot\text{OH}$ radical. Generated $\cdot\text{OH}$ can degrade the dye in aromatic ring opening pathway or N-demethylation manner. Furthermore, the holes produced on the surface of the Au particles are capable to react to water molecules to yield $\cdot\text{OH}$ [11]. Moreover, due to surface plasmon resonance effect, the intra band excited electrons of 6sp level transfer to titanium dioxide nanoparticles. The photoelectrons injected to the TiO_2 can be delivered to the oxygen molecules to form super oxide species. The radicals of super oxide as well as existed electrons at interface can cooperate to produce more $\cdot\text{OH}$. The increment of $\cdot\text{OH}$ production onto Au/T photocatalyst in comparison to T results in greatly improved photocatalytic performance of Au/T system.

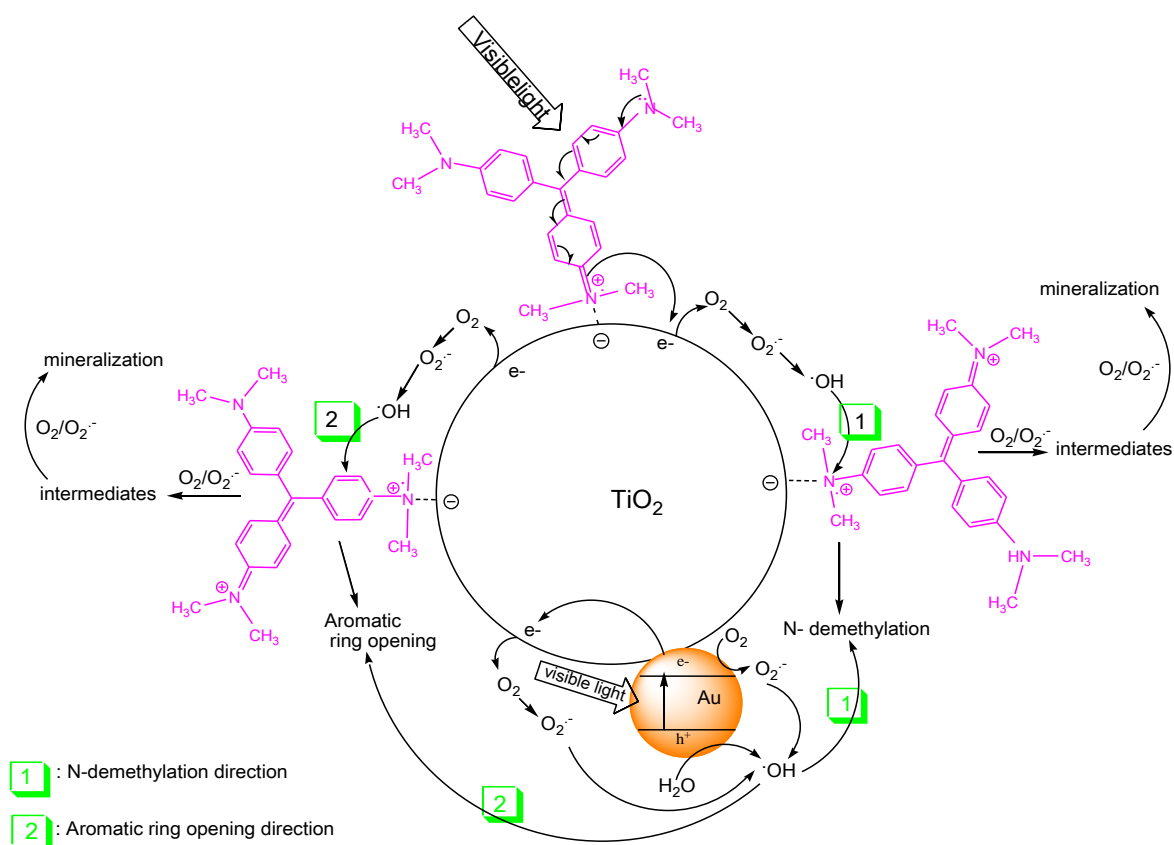


Figure 7. Schematic mechanism proposed for visible light assisted degradation of the CV dye using Au/T photocatalyst

Conclusion

Au/T nanoparticles were successfully prepared by a simple photodeposition method and used as visible light active photocatalyst towards the CV dye. The deposition of metallic Au particles on titanium dioxide surface led to appearance of a new Uv-Vis absorption band at about 550 nm, acknowledging the formation of plasmonic gold nanoparticles. During the photocatalytic reactions on the surfaces of T and Au/T nanoparticles, the absorption of the visible band at 588.5 nm decreased and a hypsochromic shift was simultaneously observed with increasing of irradiation time. This result revealed that the photodegradation of CV on the surfaces of T and Au/T photocatalysts originates from both decomposition of coherent chromophore skeleton of CV and de-methylation pathways. Au/T exhibits superior photocatalytic efficiency for decomposition of the dye when compared with the neat TiO₂. It is proposed that the much more photocatalytic efficiency of Au/T ascribes to more visible photon absorption and increased production of •OH radicals due to surface plasmon resonance effect.

Acknowledgements

Support by Nuclear Science and Technology Research Institute of AEOI is greatly appreciated.

Disclosure statement

No potential conflict of interest was reported by the authors.

ORCID

Simin Janitabar Darzi : 0000-0002-1389-917X

References

- [1] R.Krakiwicz, J. Musial, P. Bakun, M. Sychała, B. Czarzynska-Goslinska, D.T. Mlynarczyk, T. Koczorowski, L. Sobotta, B. Stanis, T. Goslinski, *Appl. Sci.*, **2021**, *11*, 8674–8706. [[CrossRef](#)], [[Google Scholar](#)], [[Publisher](#)]
- [2] S. Janitabar Darzi, A.R. Mahjoub, A. Bayat, *Int. J. Nano Dimens.*, **2016**, *7*, 33–38. [[Google Scholar](#)], [[Publisher](#)]
- [3] M. Miranzadeh, F. Afshari, B. Khataei, M.Z. Kassaei. *Adv. J. Chem. A*, **2020**, *3*, 408–421. [[CrossRef](#)], [[Google Scholar](#)], [[Publisher](#)]
- [4] A. Maria Sescu, L. Favier, D. Latic, N. Soto-Donoso, G. Ciobanu, M. Harja, *Water*, **2021**, *13*, 19–37. [[CrossRef](#)], [[Google Scholar](#)], [[Publisher](#)]
- [5] D.K. Behara, D.V. Priya Alugoti, P. Pooja Sree, *Int. J. Nano Dimens.*, **2020**, *11*, 303–311. [[Google Scholar](#)], [[Publisher](#)]
- [6] B.Z. Tian, J.L. Zhang, T.Z. Tong, F. Chen, *Appl. Catal. B*, **2008**, *79*, 394–401. [[CrossRef](#)], [[Google Scholar](#)], [[Publisher](#)]
- [7] M.A. Debeila, N.J. Coville, M.S. Scurrrell, G.R. Hearne, M.J. Witcomb, *J. Phys. Chem. B*, **2004**, *108*, 18254–18260. [[CrossRef](#)], [[Google Scholar](#)], [[Publisher](#)]
- [8] S.S. Rayalu, D. Jose, M.V. Joshi, P.A. Mangrulkar, K. Shrestha, K. Klabunde, *Appl. Catal. B: Environ.*, **2013**, *684*, 142–143. [[CrossRef](#)], [[Google Scholar](#)], [[Publisher](#)]
- [9] Y.S. Kim, P. Rai, Y.T. Yu, *Sensor. Actuator. B*, **2013**, *186*, 633–639. [[CrossRef](#)], [[Google Scholar](#)], [[Publisher](#)]
- [10] G. Kumar Naik, P. ManjariMishra, K. Parida, *Chem. Eng. J.*, **2013**, *229*, 492–497. [[CrossRef](#)], [[Google Scholar](#)], [[Publisher](#)]
- [11] M.N. Kamalasanan, S. Chandra, *Thin Solid Film.*, **1996**, *288*, 112–115. [[CrossRef](#)], [[Google Scholar](#)], [[Publisher](#)]
- [12] M. Wark, J. Tschirch, O. Bartels, D. Bahnemann, J. Rathousky., *Micropor. Mesopor. Mat.*, **2005**, *84*, 247–253. [[CrossRef](#)], [[Google Scholar](#)], [[Publisher](#)]

- [13] M. Kruk, M. Jaroniec, *Chem. Mater.*, **2001**, *13*, 3169–3183. [[CrossRef](#)], [[Google Scholar](#)], [[Publisher](#)]
- [14] A. Nilchi, S. Rasouli Garmarodi, S. Janitabar Darzi, *Sep Sci Technol.*, **2010**, *45*, 801–808. [[CrossRef](#)], [[Google Scholar](#)], [[Publisher](#)]
- [15] A.M. Putz, A. Len, C. Ianasi, C. Savii, L. Almasy, *Korean J. Chem. Eng.* **2016**, *33*, 749–754. [[CrossRef](#)], [[Google Scholar](#)], [[Publisher](#)]
- [16] C.C. Chen, H.J. Fan, C.Y. Jang, J.L. Jan, H.D. Lin, C. Lu, *J. Photochem. Photobiol. B*, **2006**, *184*, 147–154. [[CrossRef](#)], [[Google Scholar](#)], [[Publisher](#)]
- [17] B. Gao, X. Luo, H. Fu, B. Lin, Y. Chen, Z. Gu, *Mater. Res. Bull.*, **2013**, *48*, 587–594. [[CrossRef](#)], [[Google Scholar](#)], [[Publisher](#)]
- [18] C.S. Lu, F.D. Mai, C.W. Wu, R.J. Wu, C.C. Chen, *Dyes Pigm.*, **2008**, *76*, 706–713. [[CrossRef](#)], [[Google Scholar](#)], [[Publisher](#)]
- [19] M. Pelaez, P. Falaras, V. Likodimos, K. OShea, A.A.d. la Cruz, P.S.M. Dunlop, J.A. Byrne, D.D. Dionysiou, *J. Mol. Catal. A Chem.*, **2016**, *425*, 183–189. [[CrossRef](#)], [[Google Scholar](#)], [[Publisher](#)]
- [20] J. Yu, G. Dai, B. Huang, *J. Phys. Chem. C*, **2009**, *113*, 16394–16401. [[CrossRef](#)], [[Google Scholar](#)], [[Publisher](#)]
- [21] Y. Tian, T. Tatsuma, *J. Am. Chem. Soc.*, **2005**, *127*, 7632–7637. [[CrossRef](#)], [[Google Scholar](#)], [[Publisher](#)]
- [22] E.M. Cuerda-Correa, M.F. Alexandre-Franco, C. Fernández-González, *Water*, **2020**, *12*, 102–153. [[CrossRef](#)], [[Google Scholar](#)], [[Publisher](#)]

HOW TO CITE THIS ARTICLE

Simin Janitabar Darzi, Hajie Bastami, Au Decorated Mesoporous TiO₂ as a High Performance Photocatalyst towards Crystal Violet Dye, *Adv. J. Chem. A*, **2022**, 5(1), 22-30.

DOI: [10.22034/AJCA.2021.305643.1281](https://doi.org/10.22034/AJCA.2021.305643.1281)

URL: http://www.ajchem-a.com/article_139285.html